AGU100 ADVANCING EARTH AND SPACE SCIENCE

Geophysical Research Letters

RESEARCH LETTER
10.1029/2018GL080442

Key Points:
- We isolate a feedback mechanism for a partial AMOC recovery following a simulated AMOC weakening
- The heat transported by the weakening AMOC becomes more efficient as its upper branch warms
- Similar results from a 2-D model demonstrate the recovery arises through an ocean-only 2-D mechanism

Supporting Information:
- Supporting Information S1

Correspondence to:
M. D. Thomas,
matthew.thomas@yale.edu

Citation:
Thomas, M. D., & Fedorov, A. V. (2019). Mechanisms and impacts of a partial AMOC recovery under enhanced freshwater forcing. *Geophysical Research Letters*, *46*, 3308–3316. https://doi.org/10.1029/2018GL080442

Received 11 SEP 2018
Accepted 24 JAN 2019
Accepted article online 30 JAN 2019
Published online 18 MAR 2019

Mechanisms and Impacts of a Partial AMOC Recovery Under Enhanced Freshwater Forcing

M. D. Thomas[1] and A. V. Fedorov[1]

[1]Department of Geology and Geophysics, Yale University, New Haven, CT, United States

Abstract The Atlantic Meridional Overturning Circulation (AMOC) is expected to weaken in the 21st century due to increased surface buoyancy. Such AMOC changes in ocean models are often accompanied by a subsurface reduction in density. Here we perform freshwater perturbation experiments with both a 1° coupled model and an idealized zonally averaged ocean-only model to demonstrate that slow subsurface property changes (1) introduce a negative feedback that erodes the stratification and partially reinvigorates convection and the AMOC and (2) ensure the meridional heat transport weakens less than the AMOC. In the coupled model with a 0.1-Sv net freshwater flux introduced around Greenland, an initial 22% AMOC reduction over 40 years is followed by a recovery of almost half the lost strength after 400 years. The final heat transport, however, is weakened by only 7%. Similar responses in the idealized model demonstrate that 2-D ocean-only dynamics control the changes.

Plain Language Summary The Atlantic Meridional Overturning Circulation (AMOC) describes the northward upper-ocean transport and subsequent deep return flow by the currents in the Atlantic, and its heat transport is an important element of the climate. The AMOC is predicted to weaken over the 21st century, and tentative evidence suggests that it may already be slowing down. Here we use freshwater experiments with both a comprehensive climate model and an idealized numerical model to identify and explain a North Atlantic oceanic mechanism that can induce a partial recovery of the AMOC and its heat transport under climate change forcing. This mechanism operates through gradual subsurface changes in ocean properties that reduce the high-latitude vertical density gradient and allow a partial reinvigoration of the deep water formation that is necessary to sustain overturning. However, the mechanism requires that the AMOC remain active and therefore that climate change forcing remains limited.

1. Introduction

Climate predictions using numerical and theoretical models of the ocean circulation almost universally agree that the Atlantic Meridional Overturning Circulation (AMOC) will weaken over the coming century under global warming. Projections of increased future rates of glacial runoff (Intergovernmental Panel on Climate Change, 2013), rainfall (Held & Soden, 2006), and surface heating (Cheng et al., 2017; Levitus et al., 2000) near high-latitude regions of deep water formation imply the ocean there will become increasingly stratified, thereby inhibiting the convection that precedes overturning (Eden & Willebrand, 2001; Sévellec et al., 2017; Spall & Pickart, 2001; Thomas et al., 2015). The climatic consequences of a weakening AMOC on its transports of heat, freshwater, and carbon (e.g., Rhines et al., 2008), which have played key roles in bringing about past climatic events (e.g., Menviel et al., 2014; Rahmstorf, 2002), have motivated the deployment of international observing arrays that provide continuous measurements of its strength in the Atlantic Ocean, including the RAPID array (Kanzow et al., 2007) and the recent Observing the Subpolar North Atlantic Program (OSNAP) array (Lozier et al., 2017). How we interpret the future impacts of any observed and predicted AMOC trends is therefore of great importance. However, a commonly overlooked possibility is the potential for the AMOC to recover part or all of its strength following an initial climate change-induced weakening (Manabe & Stouffer, 1994). We revisit this possibility here, isolating a North Atlantic Ocean feedback mechanism for a partial AMOC recovery and, crucially, an even stronger recovery in its heat transport.

海水层化的加强不利于垂直对流

The question of whether the AMOC can recover following a climate change-induced collapse has been addressed in a number of previous "hosing" experiments using climate models, in which a large amount

下沉与回升

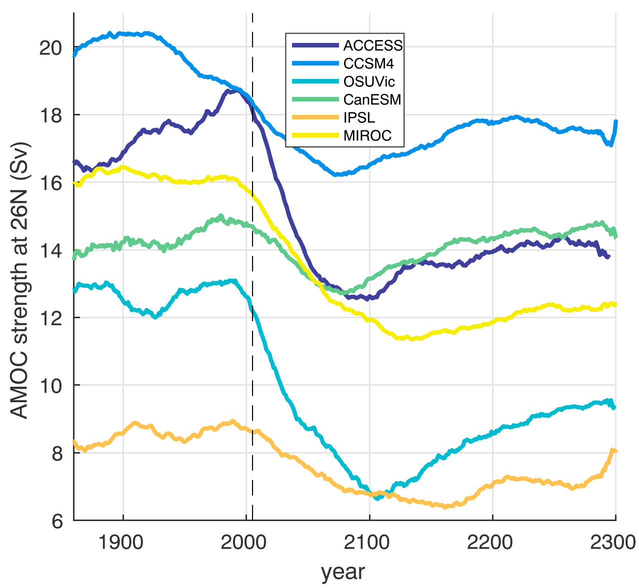

Figure 1. The AMOC strength at 26°N in all AMOCMIP ensemble members forced with the RCP4.5 emissions scenario Bakker et al. (2016). A 40-year running mean has been applied. The dashed vertical line indicates the transition from historical forcing to RCP4.5 forcing. Units are in Sverdrups (1 Sv = 10^6 m^3/s). AMOC = Atlantic Meridional Overturning Circulation; AMOCMIP = AMOC Model Intercomparison Project.

of freshwater is artificially fluxed into the North Atlantic over a finite period of time (e.g., Brunnabend & Dijkstra, 2017; den Toom et al., 2014; Jackson & Vellinga, 2013; Liu et al., 2017; Mignot et al., 2007; Vellinga & Wood, 2008; Wood et al., 2003; Zhang & Delworth, 2005). Here, however, we instead address how the AMOC will respond on multidecadal timescales to a high-latitude freshwater flux (FWF) that is both modest enough to retain an active AMOC and sustained continuously in time. Common interpretations of observed and modeled AMOC weakening trends are that it will monotonically weaken toward either a collapsed state or a new weaker steady state. However, a number of studies using models (e.g., Barreiro et al., 2008; Fedorov et al., 2007; Liu et al., 2009; Marcott et al., 2011; Mignot et al., 2007; Sévellec & Fedorov, 2015; Zhang et al., 2017) and paleotemperature reconstructions (Rasmussen & Thomsen, 2004; Ruhlemann et al., 2004) have now demonstrated that a weakening of the AMOC is accompanied by a gradual warming of the subsurface ocean. This therefore raises the possibility that the initial stratification introduced by a surface freshwater influx could be slowly eroded by subsurface changes in density, so that convection and the AMOC could be reinvigorated. This would follow a two-timescale response to both the initial stratification and the mechanism of the downward transfer of buoyancy. 这句话不知道什么意思

The possibility of an AMOC recovery under sustained but moderate climate change forcing was demonstrated by Manabe and Stouffer (1994) using a coupled ocean-atmosphere model with a 1%/year CO_2 increase maintained for 70 years before being held constant. After an initial AMOC weakening in the model, by over a factor of 2 over the first 150 years, it then fully recovered by year 500. A similar AMOC recovery after an initial weakening was recently reported from an idealized configuration of an ocean-ice general circulation model with prescribed climate change surface forcing, though the recovery in this case started after a few decades and full recovery took some thousands of years (Jansen et al., 2018). In another experiment in which the Central American seaway was artificially opened at Panama, the Atlantic freshening that occurred following exchange with the Pacific similarly induced an AMOC weakening and subsequent partial recovery starting after about 150 years (Brierley & Fedorov, 2016).

Further support for a possible future AMOC recovery under sustained and modest climate change forcing can now also be found from the Coupled Model Intercomparison Project Phase 5 (CMIP5; Cheng et al., 2013) and the more recent AMOC Model Intercomparison Project (AMOCMIP; Bakker et al., 2016). Figure 1 shows the AMOCMIP timeseries at 26°N for the historical and climate change scenarios of all long ensemble members forced with RCP4.5 forcing (Thomson et al., 2011; see supporting information, SI, text). In each of these ensemble members the AMOC first weakens before beginning to recover after ~100 years. This may demonstrate that such an AMOC recovery is a possibly robust feature among climate models. It should be noted, however, that the model run times were too short to establish whether the recovery would persist. ??

In this paper we demonstrate that the AMOC, when exposed to a sustained climate change FWF at high northern latitudes, can partially recover if the forcing does not exceed a critical threshold that would cause an AMOC collapse. We identify and isolate the mechanisms of this partial recovery in controlled freshwater experiments with a fully coupled configuration of the Community Earth System Model (CESM, Danabasoglu et al., 2012). To then test the hypotheses that the recovery can be brought about by an oceanic-only mechanism controlled by 2-D dynamics in the North Atlantic, we also use a 2-D zonally averaged Atlantic ocean-only model (Sévellec & Fedorov, 2011). We then demonstrate further how the occurrence of subsurface warming of the ocean implies an even more pronounced recovery of the Meridional Heat Transport (MHT) (Sévellec & Fedorov, 2016).

2. Numerical Models and Experiments

We performed freshwater hosing experiments with a fully coupled model and an idealized ocean-only model, in which a modest FWF that is sustained in time and does not collapse the AMOC is designed to mimic a future melting of Greenland. However, the experiments can also be considered applicable to paleo-considerations of glacial melt (e.g., of the Laurentide ice sheet) or as idealized representations of changes to the hydrological cycle or surface warming.

The coupled model we use is the CESM (version 1, Danabasoglu et al., 2012), configured according to the gx1v6 global configuration with preindustrial CO_2 levels that employs ocean, atmosphere, sea ice, and land models. The POP2 ocean model has 60 staggered vertical levels, a zonal resolution of 1°, and meridional resolution of 0.5° that decreases to 0.3° near the equator. The CAM5 atmosphere model has nominal 2° horizontal resolution. More information can be found at the UCAR website (http://www.cesm.ucar.edu/models/scientifically-supported.html). The model preindustrial control simulation has been spun-up from initial conditions for 900 years, at which point the simulation is extended for a further 250 years (presented as the model control run). Over this period the time mean AMOC strength is ~18 Sv at 26°N (1 Sv = 10^6 m^3/s), similar to the observations taken with the RAPID array (McCarthy et al., 2012). At year 900 (considered henceforth as year 0) two freshwater experiments were performed, in which a total FWF of magnitude of 0.1 and 0.15 Sv was added uniformly into the surface layer of the grid cells immediately surrounding the lower half of Greenland (Figure S1a). These fluxes were then maintained throughout the simulations for 630 years. We conserve freshwater in the model by balancing the positive flux by an evenly distributed removal of freshwater from the rest of the global ocean surface, done so as to both better compare to the 2-D model (described below) and also to allow the FWF to represent a change in the hydrological cycle (Held & Soden, 2006).

The imposed FWFs can be compared to an estimate that Greenland meltwater will reach ~0.067 Sv by 2100 if rates of melting continue at the same observed acceleration (Swingedouw et al., 2013). However, while changes in freshwater forcing cannot be considered to induce the same response as a change in surface warming, our experiments are intended to provide an idealized representation of the combined effect of future forcing from meltwater, changes in hydrological cycle and heat fluxes.

We also use an idealized zonally averaged ocean-only model of the Atlantic and Southern Oceans (Sévellec & Fedorov, 2011). The model has prognostic equations for temperature and salinity, which each includes terms (with adjustable coefficients) for advection, isopycnal and diapycnal diffusion, convection, and surface forcing. Idealized forcing terms take the form of mixed surface boundary conditions: surface temperature restoring (Figure S2a), fixed surface salinity flux (Figure S2b), and wind stress (Figure S2c). Convection occurs as an instantaneous adjustment to an unstable water column. Density is calculated according to a linear equation of state, and the pressure field is hydrostatic. Meridional velocities are diagnosed according to the meridional pressure gradient scaled by a linear friction coefficient, as well as Ekman transport and eddy-induced velocities (Gent & Mcwilliams, 1990). The model latitude range is 66°S to 66°N with a horizontal resolution of ~4.5° and 15 staggered vertical levels. Coefficients for horizontal and vertical diffusivity are 10^3 and 10^{-4} m^2/s, respectively, unless stated otherwise. Assuming the Atlantic basin width of 5,100 km, transport fluxes can be calculated in units of Sverdrups. (See Sévellec & Fedorov, 2011, for a full description of the model terms, parameters, and forcing profiles, as well as discussion of assumptions such as scaling the AMOC with meridional pressure gradients). Note that while surface temperature restoring provides a negative feedback that helps maintain model stability, it may also constrain how the temperature can respond to freshwater forcing. The conclusions, however, are not sensitive to a doubling or halving of the default temperature restoring timescale of 1/66 per day.

The 2-D model serves a number of valuable purposes in this study: (1) It allows us to verify that the recovery mechanism is an ocean-only mechanism that is not related to atmospheric feedbacks and confined to the North Atlantic; (2) it can be used to verify that the AMOC and MHT responses to a high-latitude FWF are driven by two-dimensional dynamics on a depth-latitude plane; (3) it allows us to more easily explore the sensitivity of the AMOC response to different model parameters and FWFs, which is not possible with the expensive CESM configuration; and (4) the model is simple enough to explore the above points while retaining important dynamics such as convection.

We employ the well tested 2-D model control parameters reported by Sévellec and Fedorov (2011), in which the basin-wide maximum AMOC strength (see SI text) is realistic (Figure 2c). Hosing experiments have then been performed for 5,000 years, using a Gaussian latitude-profile FWF centered at 60°N and spanning the subpolar gyre (Figure S1b). Freshwater is conserved throughout the duration of the runs by balancing the positive influx at the surface of the rest of the model, a necessary step in order to produce realistic results.

10.1029/2018GL080442

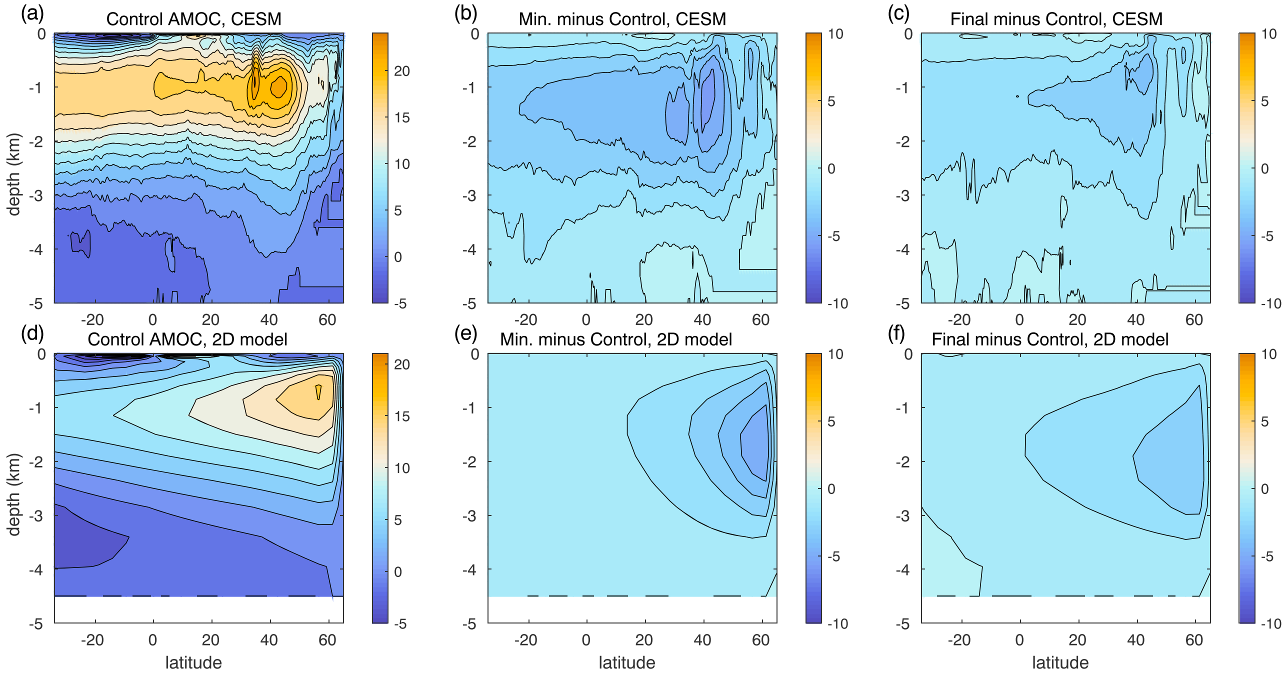

Figure 2. AMOC Eulerian streamfunctions for (a–c) CESM and (d–f) the 2-D model. (a, d) Time mean stream function in the control experiment, and its change in perturbation experiments relative to the control (b, e) when the AMOC strength is minimum and (c, f) when the AMOC reaches a quasi-equilibrium (years 400–420). The CESM and 2-D model experiments use 0.1 Sv and 25 cm/year of freshwater forcing, respectively. Units are in Sverdrups. AMOC = Atlantic Meridional Overturning Circulation; CESM = Community Earth System Model.

Experiments using peak FWFs of 25 and 35 cm/year (equivalent to ~0.08 and ~0.11 Sv, respectively, when integrated over the anomaly profiles) have been applied since their results resemble the coupled model freshwater experiments. Sensitivity experiments to FWF have then included a range of fluxes between 10 and 90 cm/year (~0.03 and ~0.28 Sv, respectively). Further sensitivity tests to FWF were also conducted with different values of vertical diffusivity and Southern Ocean wind stress, as reported later.

3. Results

We first demonstrate how the AMOC responds in the model FWF experiments in both the fully coupled configuration of CESM and in the 2-D model (see methods). We then discuss the ocean property changes and mechanisms that are responsible for the AMOC recovery and the stronger reinvigoration of the MHT (see SI text for calculations of the AMOC, MHT, and mixed layer depth (MLD); Marshall et al., 1993; Schmidtko et al., 2013; Thomas & Fedorov, 2017).

3.1. AMOC Response to a Moderate FWF

Figure 3a shows the AMOC time series of the control and the two FWF experiments at 46°N in the CESM configuration, 40-year smoothed to highlight the multidecadal changes. As expected from previous studies using similar magnitude FWFs (Barreiro et al., 2008; Smith et al., 2014; Swingedouw et al., 2013), the model AMOC in the experiments initially weakens in response to the increase in high-latitude stratification, decreasing in the 0.1-Sv FWF run from ~22 to ~17 Sv (at 46°N) over the first ~40 years at a rate of ~0.12 Sv/year. For context, this rate is close to an observed estimate of 0.13 Sv/year derived from satellite and cable data at 26°N between 1993 and 2014, although this trend was found to be not significant and might reflect natural ocean variability (Frajka-Williams, 2015).

After 40 years the model AMOC starts to recover, which supports our hypothesis and, as discussed below, is consistent with a gradual subsurface erosion of the high-latitude stratification that partly reinvigorates deep convection. Recovery continues for the next 350 years, strengthening by a total of ~2.2 Sv until a new near-steady state is reached. To test the sensitivity of the AMOC recovery to the strength of the FWF, the experiment has been repeated using a FWF of 0.15 Sv. This flux induces the same pattern of weakening and recovery, reaching a ~1 Sv weaker AMOC strength than in the 0.1-Sv FWF experiment (Figure 3a).

淡水的注入会减弱AMOC

MHT=meridional heat transport 径向热输运

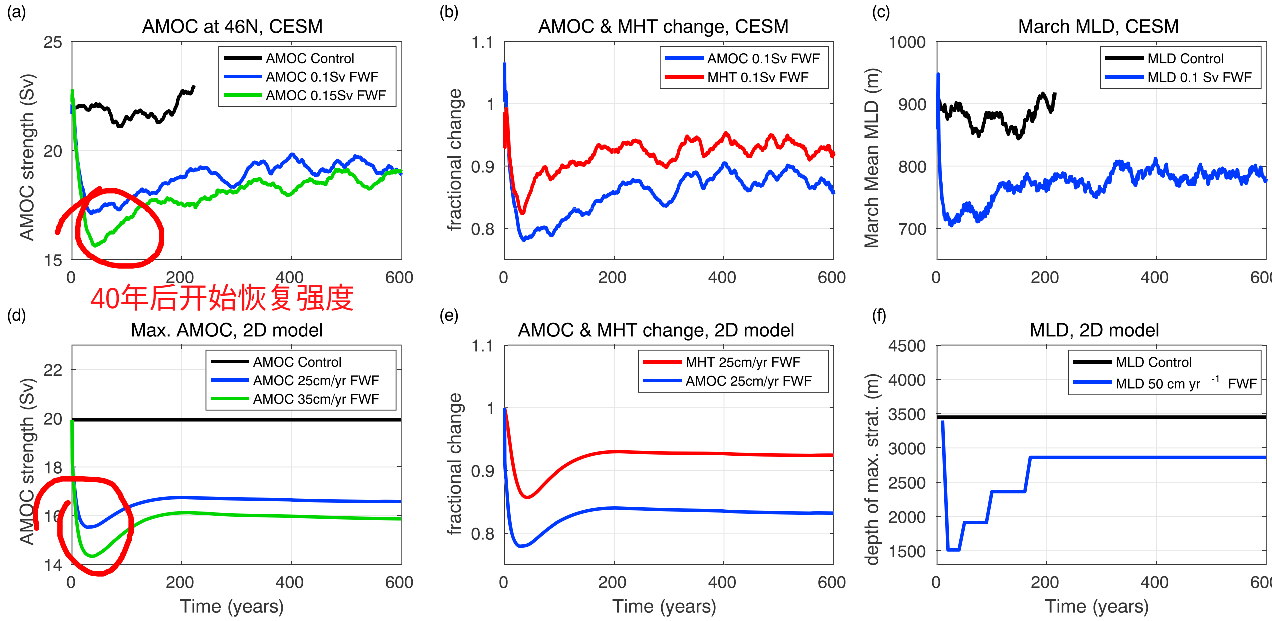

Figure 3. (a–c) CESM and (d–f) 2-D model time series for several freshwater forcing experiments: (a, d) the maximum control and FWF experiment AMOC strengths, (b, e) the normalized AMOC and MHT strengths of the 0.1-Sv FWF CESM and 25-cm/year 2-D model experiments, calculated relative to the time mean control strengths (21.9 Sv and 0.63 PW for CESM at 46°N, respectively, and 19.9 Sv and 0.62 PW for the 2-D model respectively), and (c, f) the average mixed layer depth within the convection regions. A 40-year smoothing was applied. The AMOC strength includes parameterized eddy contributions. Mixed layers are calculated as the March mean depth within convection regions (CESM) and as the depth of maximum density stratification in the downwelling region (2-D model). AMOC = Atlantic Meridional Overturning Circulation; CESM = Community Earth System Model; FWF = freshwater flux; MLD = mixed layer depth.

To test sensitivity to the initial conditions, the 0.1-Sv FWF experiment was also repeated starting at an earlier period of the control simulation, and the results were closely reproduced (Figure S3). This experiment was run for 950 years to verify that the AMOC reached a new near-equilibrium state. It is noteworthy that in numerical experiments using weakly enhanced surface warming (Jansen et al., 2018) and CO_2 forcing (Manabe & Stouffer, 1994) the simulated AMOC can make an eventual full recovery. Consistent with Jansen et al. (2018), we suggest that our North Atlantic mechanism controls an initial centennial timescale AMOC adjustment, while longer timescale changes are brought about by Southern Ocean adjustments that are excluded from our experimental design.

We now use the 2-D model FWF experiments to test whether both the initial weakening and eventual recovery can be largely explained according to two dimensional ocean-only dynamics. The AMOC response in the simpler model is qualitatively very similar to that of the coupled model (Figures 3a and 3d), with a timescale before recovery of about 35 years and an eventual 1.5-Sv recovery from a minimum value of 15.5 Sv in the 25-cm/year experiment. Despite a faster recovery timescale in the 2-D model, the agreement is striking given the large differences between the two models. Changes in the stream function in both models, displayed for both the minimum value (years 35–55 average; Figures 2b and 2e) and its near-equilibrium state (years 400–420 average; Figures 2c and 2f), reveal reductions in AMOC strength that are similarly produced in both models. The high northern latitude-centered AMOC changes are consistent with a buoyancy-driven AMOC change (Eden & Willebrand, 2001).

To test that the AMOC response to increased FWF is a consistent response across parameter space in the 2-D model, we have modified the magnitude of the FWF, the surface temperature restoring timescale, the horizontal diffusivity, vertical diffusivity (Figure S4), and the wind stress over the Southern Ocean (Figure S4). See Figures S1c and S2c for the surface wind stress profiles and Sévellec and Fedorov (2011) for its application in the model equations. We find that the occurrence of an AMOC recovery is robust across a broad range of parameters (that provide reasonable temperature, salinity, and density fields and retain an active AMOC). However, the time when recovery begins (ranging from ~30–300 years), the minimum AMOC strength before recovery (down to ~8 Sv), the timescale to equilibrium, and the recovery magnitude do depend on the parameters, indicating that model dependency is a factor. Of these, the first two are most

淡水灌注实验下不同变量最小值的敏感度图(和控制实验相比)

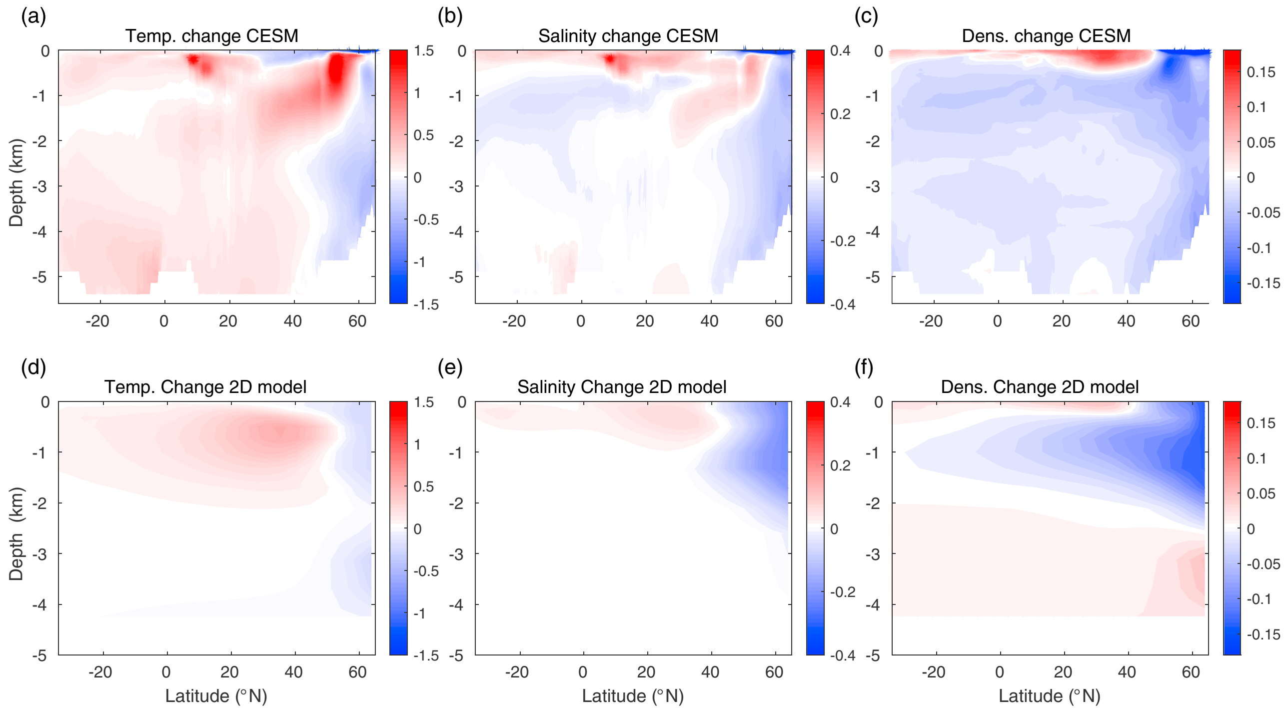

Figure 4. The Atlantic zonally averaged (a–c) 0.1-Sv Community Earth System Model (CESM) and (d–f) 25-cm/year 2-D model changes in (a, d) temperature (°C), (b, e) salinity, and (c, f) density (kg/m^3), calculated at the time of minimum AMOC strength (years 30–50 average) relative to the time mean control values (minimum minus control).

sensitive to the magnitude of the FWF (discussed below), and the latter two are most strongly affected by the magnitudes of the vertical diffusivity and Southern Ocean wind stress (Figure S4): Increased vertical diffusivity leads to a longer equilibrium timescale and a weaker recovery relative to the peak minimum and vice versa for the wind stress (see section 3.2 for a hypothesis to explain this result). Such model sensitivities may explain the different responses to forcing changes exhibited between the AMOCMIP model members (Figure 1 Bakker et al., 2016) and their differences to the faster recovery time in our CESM configuration (see Swingedouw et al., 2013, for an evaluation of model dependent responses to 0.1-Sv hosing).

Figure S4 shows the 2-D model sensitivity to increasing values of freshwater in each of the 2-D model parameter-sensitivity experiments. We focus on the experiment with default parameter settings shown in the middle subpanel (Figure S4e). While the shape of the decline and recovery is similar across all forcing strengths at or below 70 cm/year, the timescale to the AMOC minimum increases with freshwater forcing. This is likely because larger subsurface changes must first develop to overcome a larger stratification. The AMOC state has a sudden bifurcation point, collapsing at ~70.1 cm/year. At the freshwater forcing value of 70 cm/year the AMOC takes ~200 years before a recovery occurs. We note that this strong sensitivity to the freshwater forcing happens only in a narrow range of FWFs just before the bifurcation point. At a stronger forcing than 70.1 cm/year the AMOC collapses increasingly rapidly. Similar behavior in response to stronger FWF forcing also occurs when employing different model parameter values for vertical diffusivity or Southern Ocean wind stress, though each has a different FWF value at the bifurcation (Figure S4).

3.2. Mechanisms of AMOC Recovery and Impact on MHT

To elucidate the mechanisms of the AMOC recovery in the two models, we show changes in the zonal mean temperature, salinity, and density fields at the time of minimum AMOC (Figure 4), as well as their evolution over the first 90 years following increased freshwater forcing (Figures S5 and S6). We then compare these to the model high-latitude March-mean MLD changes in the deep convection regions (see SI text), which has previously been shown to be a good indicator of convective mixing and deep water formation on decadal to multidecadal timescales (e.g., Eden & Willebrand, 2001; Spall & Pickart, 2001; Thomas et al., 2015). The initial freshening is confined to the upper ocean at high latitude (Figures S5 and S6) and induces a rapid weakening in convection, as indicated by a shoaling of the high-latitude MLD (Figures 3c and 3f), and a

由于MHT减弱,表层水温度降低

由于向下的对流减弱，次表层水温度升高

weakening of the AMOC (Figures 3a and 3d). Similar to previous findings (Barreiro et al., 2008; Fedorov et al., 2007; Liu et al., 2009; Marcott et al., 2011; Mignot et al., 2007; Sévellec & Fedorov, 2015), this is accompanied at first by high-latitude surface cooling due to a weakened northward MHT and subsurface warming possibly due to weaker convection (Figures S5 and S6). Initially-small in magnitude, subsurface temperature anomalies in both models then grow and move southward, being replaced over the first decade by a high-latitude cooling signature at all depths (Figures 4a, 3d, S5, and S6). Along with downward diffusion of the surface signature, the development of the high-latitude cooling is largely a consequence of the still-active AMOC that advects and mixes the surface signal downward (Figure S7). Subsurface freshening similarly takes place at high latitudes (Figures 4b, 4e, S5, and S6), countering the subsurface cooling and dominating density changes (Figures 4c and 4f). The subsurface subtropical gyre then continues to warm, either because of weaker northward heat transport along the subsurface pathway out of the subtropics (Mignot et al., 2007), leading to heat convergence, or because of weakened subtropical upwelling under a weaker AMOC (Manabe & Stouffer, 1994). The result of the property changes in both models is the development of a subsurface tongue of low density water at all latitudes that is controlled by both freshening at high latitudes and warming at low latitudes. After ~40 years into the simulations, changes in the high-latitude vertical density gradient bring about an AMOC recovery as the signature propagates southward.

This recovery mechanism, brought about by reduction in subsurface density, may help explain the AMOC responses to increased Southern Ocean wind stress and increased diffusivity, which respectively enhance and suppress the recovery magnitude and timescales (as mentioned in the previous subsection; Figure S4). While increases in both parameters act to strengthen the AMOC, which might be expected to enhance the recovery through more rapid development of the subsurface signature, a higher diffusivity may hinder its development by diffusing away the signal. Further work is needed, however, to test this hypothesis.

Of greater importance for the climate is the response of the MHT to the FWF. Subtropical warming, while strongest in the subsurface, occurs within the northward branch of the AMOC in both models. Therefore, although the AMOC weakens following increased freshwater input, it becomes more efficient by transporting warmer water (Sévellec & Fedorov, 2016). Accordingly, in the two models we find that the relative weakening of the MHT is less pronounced than that of the AMOC volume transport, when calculated relative to their control mean strengths (Figures 3b and 3d). This is the case at all latitudes where warming occurs, including northward and southward of the subtropics, and is therefore not related to the transport of heat by the gyre. This is further evidenced by the similar MHT response in the 2-D model, in which there is only an AMOC change.

4. Conclusions

Using freshwater experiments applied to a fully coupled model and a zonally averaged ocean model, in which freshwater was artificially fluxed into the surface of the high-latitude North Atlantic, we have demonstrated that the AMOC, and particularly its associated heat transport, can partially recover under sustained high-latitude climate change forcing. A similarity in the responses of the two models to freshwater forcing demonstrates that the recovery is an oceanic-only mechanism that emerges in a 2-D framework. However, it requires that the ocean retains an active AMOC, necessitating that greenhouse gas emissions do not exceed a threshold magnitude. In climate models (Bakker et al., 2016; Cheng et al., 2013) this critical threshold is exceeded in all projections with the RCP8.5 emissions.

In our freshwater forcing experiments the onset of a recovery is due to a negative climate feedback that can initiate the recovery after some 40 years of initial weakening. The mechanism is brought about by gradual high-latitude subsurface freshening, caused by the downward advection and mixing of freshwater by the still-active AMOC (Figures 4b and 4e). This erodes the initial stratification imposed by surface freshening, thus reinvigorating convection (Figures 3c and 3f) and the AMOC (Figures 3a and 3d). Subsequent subsurface subtropical warming (Figures 4a and 4d) then ensures that the MHT weakens less than the AMOC volume transport (Figures 3b and 3e). Although the magnitudes of the initial weakening, the subsequent recovery, and the timescale to recovery are all sensitive to the choices of the 2-D model parameters, the occurrence of a recovery is a robust feature across parameter space (Figure S4). The mechanism of recovery in our experiments, through the downward transfer of high-latitude surface freshwater, is different to our initial hypothesis that subsurface warming reinvigorates convection. Further work is needed to assess whether future surface heating applied to the subolar North Atlantic would yield similar results following the downward transfer of warm surface temperatures, such as may be occurring in AMOCMIP (Bakker et al., 2016).

In CESM, forced with a 0.1-Sv FWF that is artificially injected around southern Greenland, a minimum AMOC weakening that peaks at a 22% reduction eventually comes into an equilibrium state in which the MHT is weakened by only 7%. One possible implication of this recovery can be seen in the relative changes in sea surface temperature between the AMOC minimum and its final equilibrated state (Figure S8). In the 0.1-Sv FWF CESM experiment, large sea surface temperature increases of up to 2°C occur in the North Atlantic and Nordic Seas following the recovery; however, it is not clear to what extent this is related to coupled atmosphere-ocean feedbacks (e.g., Zhang et al., 2010) and requires future research. Our results also challenge the commonly held perception of a one-to-one relationship between the AMOC and the MHT, which does not account for possible relative changes in the vertical profiles of temperature and velocity. Finally, the model temperature and salinity changes that prime the AMOC recovery resemble those observed to have taken place in the Atlantic Ocean with depth during the second half of the twentieth century (Curry et al., 2003; Levitus et al., 2000). Future work will be required to assess if these changes are due to the mechanisms we describe here and whether they could bring about a partial recovery during a potential AMOC decline (Caesar et al., 2018; Thornalley et al., 2018).

Acknowledgments
This research is supported by grants from the National Science Foundation (OCE-1756682 and OPP-1741847) and the Guggenheim fellowship to A. V. F. We would like to acknowledge high-performance computing support from Cheyenne (doi:10.5065/D6RX99HX) and Yellowstone (ark:/85065/d7wd3xhc), provided by NCAR's Computational and Information Systems Laboratory, sponsored by the National Science Foundation. The authors are extremely grateful to Florian Sévellec for help with the zonally averaged model, Pepijn Bakker for providing data from AMOCMIP, Cecelia Bitz for help on applying freshwater fluxes in CESM, and to Kaylea Nelson for help with CESM and the Yale computing resources. Constructive comments from two reviewers are gratefully acknowledged. All model data produced for this manuscript are stored on Zenodo, accessible using the Zenodo website (DOI 10.5281/zenodo.2540877).

References

Bakker, P., Schmittner, A., Lenaerts, J. T. M., Abe-Ouchi, A., Bi, D., van den Broeke, M. R., et al. (2016). Fate of the Atlantic Meridional Overturning Circulation: Strong decline under continued warming and Greenland melting. *Geophysical Research Letters*, *43*, 12,252–12,260. https://doi.org/10.1002/2016GL070457

Barreiro, M., Fedorov, A., Pacanowski, R., & Philander, S. G. (2008). Abrupt climate changes: How freshening of the northern Atlantic affects the thermohaline and wind-driven oceanic circulations. *Annual Review of Earth and Planetary Sciences*, *36*, 33–58. https://doi.org/10.1146/annurev.earth.36.090507.143219

Brierley, C. M., & Fedorov, A. V. (2016). Comparing the impacts of Miocene-Pliocene changes in inter-ocean gateways on climate: Central American seaway, Bering strait, and Indonesia. *Earth and Planetary Science Letters*, *444*, 116–130. https://doi.org/10.1016/j.epsl.2016.03.010

Brunnabend, S. E., & Dijkstra, H. A. (2017). Asymmetric response of the Atlantic Meridional Ocean Circulation to freshwater anomalies in a strongly-eddying global ocean model. *Tellus Series A-dynamic Meteorology and Oceanography*, *69*, 1299283. https://doi.org/10.1080/16000870.2017.1299283

Caesar, L., Rahmstorf, S., Robinson, A., Feulner, G., & Saba, V. (2018). Observed fingerprint of a weakening Atlantic Ocean overturning circulation. *Nature*, *556*(7700), 191–196. https://doi.org/10.1038/s41586-018-0006-5

Cheng, W., Chiang, J. C. H., & Zhang, D. X. (2013). Atlantic Meridional Overturning Circulation (AMOC) in CMIP5 models: RCP and historical simulations. *Journal of Climate*, *26*(18), 7187–7197. https://doi.org/10.1175/JCLI-D-12-00496.1

Cheng, L. J., Trenberth, K. E., Fasullo, J., Boyer, T., Abraham, J., & Zhu, J. (2017). Improved estimates of ocean heat content from 1960 to 2015. *Science Advances*, *3*(3), e1601545. https://doi.org/10.1126/sciadv.1601545

Curry, R., Dickson, B., & Yashayaev, I. (2003). A change in the freshwater balance of the Atlantic Ocean over the past four decades. *Nature*, *426*(6968), 826–829. https://doi.org/10.1038/nature02206

Danabasoglu, G., Bates, S. C., Briegleb, B. P., Jayne, S. R., Jochum, M., Large, W. G., et al. (2012). The CCSM4 ocean component. *Journal of Climate*, *25*(5), 1361–1389. https://doi.org/10.1175/JCLI-D-11-00091.1

den Toom, M., Dijkstra, H. A., Weijer, W., Hecht, M. W., Maltrud, M. E., & van Sebille, E. (2014). Response of a strongly eddying global ocean to North Atlantic freshwater perturbations. *Journal of Physical Oceanography*, *44*(2), 464–481. https://doi.org/10.1175/JPO-D-12-0155.1

Eden, C., & Willebrand, J. (2001). Mechanism of interannual to decadal variability of the North Atlantic circulation. *Journal Climate*, *14*(10), 2266–2280.

Fedorov, A., Barreiro, M., Boccaletti, G., Pacanowski, R., & Philander, S. G. (2007). The freshening of surface waters in high latitudes: Effects on the thermohaline and wind-driven circulations. *Journal of Physical Oceanography*, *37*(4), 896–907. https://doi.org/10.1175/JPO3033.1

Frajka-Williams, E. (2015). Estimating the Atlantic overturning at 26°N using satellite altimetry and cable measurements. *Geophysical Research Letters*, *42*, 3458–3464. https://doi.org/10.1002/2015GL063220

Gent, P. R., & Mcwilliams, J. C. (1990). Isopycnal mixing in ocean circulation models. *Journal of Physical Oceanography*, *20*(1), 150–155. https://doi.org/10.1175/1520-0485(1990)020<0150:IMIOCM>2.0.CO;2

Held, I. M., & Soden, B. J. (2006). Robust responses of the hydrological cycle to global warming. *Journal of Climate*, *19*(21), 5686–5699. https://doi.org/10.1175/JCLI3990.1

Intergovernmental Panel on Climate Change (2013). *Climate change 2013: The physical science basis. Contribution of Working Group I to the Fifth Assessment Report of the Intergovernmental Panel on Climate Change*. Cambridge, United Kingdom and New York, NY: Cambridge University Press. ISBN ISBN 978-1-107-66182-0.10.1017/CBO9781107415324, URL www.climatechange2013.org

Jackson, L., & Vellinga, M. (2013). Multidecadal to centennial variability of the AMOC:HadCM3 and a perturbed physics ensemble. *Journal Climate*, *26*, 2390–2407.

Jansen, M., Nadeau, L.-P., & Merlis, T. M. (2018). Transient versus equilibrium response of the ocean's overturning circulation to warming. *Journal Climate*, *31*, 5147–5163.

Kanzow, T., Cunningham, S. A., Rayner, D., Hirschi, J. J. M., Johns, W. E., Baringer, M. O., et al. (2007). Observed flow compensation associated with the MOC at 26.5 degrees N in the Atlantic. *Science*, *317*(5840), 938–941.

Levitus, S., Antonov, J. I., Boyer, T. P., & Stephens, C. (2000). Warming of the world ocean. *Science*, *287*(5461), 2225–2229.

Liu, Z., Otto-Bliesner, B. L., He, F., Brady, E. C., Tomas, R., Clark, P. U., et al. (2009). Transient simulation of last deglaciation with a new mechanism for Bolling-Allerod warming. *Science*, *325*(5938), 310–314. https://doi.org/10.1126/science.1171041

Liu, W., Xie, S. P., Liu, Z. Y., & Zhu, J. (2017). Overlooked possibility of a collapsed Atlantic Meridional Overturning Circulation in warming climate. *Science Advances*, *3*(1), e1601666. https://doi.org/10.1126/sciadv.1601666

Lozier, M. S., Bacon, S., Bower, A. S., Cunningham, S. A., de Jong, M. F., de Steur, L., et al. (2017). Overturning in the subpolar North Atlantic program a new international ocean observing system. *Bulletin of the American Meteorological Society*, *98*(4), 737–752. https://doi.org/10.1175/BAMS-D-16-0057.1

Manabe, S., & Stouffer, R. J. (1994). Multiple-century response of a coupled ocean-atmosphere model to an increase of atmospheric carbon-dioxide. *Journal of Climate*, *7*(1), 5–23. https://doi.org/10.1175/1520-0442(1994)007<0005:MCROAC>2.0.CO;2

Marcott, S. A., Clark, P. U., Padman, L., Klinkhammer, G. P., Springer, S. R., Liu, Z. Y., et al. (2011). Ice-shelf collapse from subsurface warming as a trigger for Heinrich events. *Proceedings of the National Academy of Sciences of the United States of America*, *108*(33), 13,415–13,419. https://doi.org/10.1073/pnas.1104772108

Marshall, J. C., Nurser, A. J. G., & Williams, R. G. (1993). Inferring the subduction rate and period over the North-Atlantic. *Journal of Physical Oceanography*, *23*(7), 1315–1329. https://doi.org/10.1175/1520-0485(1993)023<1315:ITSRAP>2.0.CO;2

McCarthy, G., Frajka-Williams, E., Johns, W. E., Baringer, M. O., Meinen, C. S., Bryden, H. L., et al. (2012). Observed interannual variability of the Atlantic Meridional Overturning Circulation at 26.5 degrees N. *Geophysical Research Letters*, *39*, L19609. https://doi.org/10.1029/2012GL052933

Menviel, L., Timmermann, A., Friedrich, T., & England, M. H. (2014). Hindcasting the continuum of dansgaard-oeschger variability: Mechanisms, patterns and timing. *Climate of the Past*, *10*(1), 63–77. https://doi.org/10.5194/cp-10-63-2014

Mignot, J., Ganopolski, A., & Levermann, A. (2007). Atlantic subsurface temperatures: Response to a shutdown of the overturning circulation and consequences for its recovery. *Journal of Climate*, *20*(19), 4884–4898. https://doi.org/10.1175/JCLI4280.1

Rahmstorf, S. (2002). Ocean circulation and climate during the past 120,000 years. *Nature*, *419*(6903), 207–214. https://doi.org/10.1038/nature01090

Rasmussen, T. L., & Thomsen, E. (2004). The role of the North Atlantic drift in the millennial timescale glacial climate fluctuations. *Palaeogeography Palaeoclimatology Palaeoecology*, *210*(1), 101–116. https://doi.org/10.1016/j.palaeo.2004.04.005

Rhines, P., Häkkinen, S., & Josey, S. A. (2008). Is the oceanic heat transport significant in the climate system? In R. R. Dickson, J. Meincke, & P. Rhines (Eds.), *Arctic-subarctic ocean fluxes: Defining the role of the Northern Seas in climate* (pp. 111–130). Dordrecht, Netherlands: Springer.

Ruhlemann, C., Mulitza, S., Lohmann, G., Paul, A., Prange, M., & Wefer, G. (2004). Intermediate depth warming in the tropical Atlantic related to weakened thermohaline circulation: Combining paleoclimate data and modeling results for the last deglaciation. *Paleoceanography*, *19*, PA1025. https://doi.org/10.1029/2003PA000948

Schmidtko, S., Johnson, G. C., & Lyman, J. M. (2013). MIMOC: A global monthly isopycnal upper-ocean climatology with mixed layers. *Journal of Geophysical Research: Oceans*, *118*, 1658–1672. https://doi.org/10.1002/jgrc.20122

Sévellec, F., & Fedorov, A. V. (2011). Stability of the Atlantic Meridional Overturning Circulation and stratification in a zonally averaged ocean model: Effects of freshwater flux, southern ocean winds, and diapycnal diffusion. *Deep-sea Research Part Ii-topical Studies In Oceanography*, *58*(17-18), 1927–1943. https://doi.org/10.1016/j.dsr2.2010.10.070

Sévellec, F., & Fedorov, A. V. (2015). Optimal excitation of AMOC decadal variability: Links to the subpolar ocean. *Progress In Oceanography*, *132*, 287–304. https://doi.org/10.1016/j.pocean.2014.02.006

Sévellec, F., & Fedorov, A. V. (2016). AMOC sensitivity to surface buoyancy fluxes: Stronger ocean meridional heat transport with a weaker volume transport? *Climate Dynamics*, *47*(5-6), 1497–1513. https://doi.org/10.1007/s00382-015-2915-4

Sévellec, F., Fedorov, A. V., & Liu, W. (2017). Arctic sea-ice decline weakens the Atlantic Meridional Overturning Circulation. *Nature Climate Change*, *7*(8), 604–610. https://doi.org/10.1038/NCLIMATE3353

Smith, R. S., Sutton, R., & Gregory, J. M. (2014). The impact of salinity perturbations on the future uptake of heat by the Atlantic Ocean. *Geophysical Research Letters*, *41*, 9072–9079. https://doi.org/10.1002/2014GL062169

Spall, M. A., & Pickart, R. S. (2001). Where does dense water sink? A subpolar gyre example. *Journal of Physical Oceanography*, *31*, 810–826.

Swingedouw, D., Rodehacke, C. B., Behrens, E., Menary, M., Olsen, S. M., Gao, Y. Q., et al. (2013). Decadal fingerprints of freshwater discharge around Greenland in a multi-model ensemble. *Climate Dynamics*, *41*(3-4), 695–720. https://doi.org/10.1007/s00382-012-1479-9

Thomas, M. D., & Fedorov, A. V. (2017). The eastern subtropical pacific origin of the equatorial cold bias in climate models: A Lagrangian perspective. *Journal of Climate*, *30*(15), 5885–5900. https://doi.org/10.1175/JCLI-D-16-0819.1

Thomas, M. D., Treguier, A.-M., Blanke, B., Deshayes, J., & Voldoire, A. (2015). A Lagrangian method to isolate the impacts of mixed layer subduction on the meridional overturning circulation in a numerical model. *Journal Climate*, *28*(19), 7503–7517. https://doi.org/10.1175/JCLI-D-14-00631.1

Thomson, A. M., Calvin, K. V., Smith, S. J., Kyle, G. P., Volke, A., Patel, P., et al. (2011). RCP4.5: A pathway for stabilization of radiative forcing by 2100. *Climatic Change*, *109*(1-2), 77–94. https://doi.org/10.1007/s10584-011-0151-4

Thornalley, D. J. R., Oppo, D. W., Ortega, P., Robson, J. I., Brierley, C. M., Davis, R., et al. (2018). Anomalously weak Labrador Sea convection and Atlantic overturning during the past 150 years. *Nature*, *556*(7700), 227. https://doi.org/10.1038/s41586-018-0007-4

Vellinga, M., & Wood, R. A. (2008). Impacts of thermohaline circulation shutdown in the twenty-first century. *Climatic Change*, *91*(1-2), 43–63. https://doi.org/10.1007/s10584-006-9146-y

Wood, R. A., Vellinga, M., & Thorpe, R. (2003). Global warming and thermohaline circulation stability. *Philosophical Transactions of the Royal Society A*, *361*(1810), 1961–1974.

Zhang, R., & Delworth, T. L. (2005). Simulated tropical response to a substantial weakening of the Atlantic thermohaline circulation. *Journal of Climate*, *18*(12), 1853–1860. https://doi.org/10.1175/JCLI3460.1

Zhang, R., Kang, S. M., & Held, I. M. (2010). Sensitivity of climate change induced by the weakening of the Atlantic Meridional Overturning Circulation to cloud feedback. *Journal of Climate*, *23*(2), 378–389. https://doi.org/10.1175/2009JCLI3118.1

Zhang, X., Knorr, G., Lohmann, G., & Barker, S. (2017). Abrupt North Atlantic circulation changes in response to gradual CO_2 forcing in a glacial climate state. *Nature Geoscience*, *10*(7), 518. https://doi.org/10.1038/NGEO2974